ISSN No.: 2455-6130
Special Issue – RAISE2024, 2025,, pp. 26-36

website: www.ijoetr.com

International Journal of Emerging Trends in Research

Experimental Investigation of Machining Performance of Micro Groove Textured High Speed Steel Tools During Turning of SS 316 L under Dry Environment Conditions

Dr. Balasubramanyam. N[1*], Mrs.B. Rajitha[2]

[1]*Dept. of Mechanical Engineering, S.V.University College of Engineering Tirupati, Andhra Pradesh*
[2]*Dept.of Physics, Sri Padmavathi Mahila Visvavidyalayam Tirupati, Andhra Pradesh*
* Corresponding author. E-mail: balu.phd28@gmail.com

Abstract

This research investigates the machining performance of micro-groove textured high-speed steel (HSS) tools during the turning of SS 316L under dry conditions. Surface texturing on cutting tools is a promising approach to enhance cutting performance by reducing friction and wear. In this study, micro-grooves were created on HSS tools, and their performance was evaluated in terms of cutting force, surface roughness, tool wear, and temperature rise during the dry turning of stainless steel 316L (SS 316L). The present study is conducted to determine the machining performance of a micro-groove-textured high-speed steel (HSS) tool during the turning of austenitic stainless steel (SS) 316 L in a dry environment. Dry turning experiments are conducted at a combination of varied parameters such as cutting speed, feed, and depth of cut based on the Taguchi L9 orthogonal array. A detailed study was conducted on chip morphology and chip compression ratio to understand the effect of machining parameters on the micro-textured HSS tool's performance. The optimum levels of these machining parameters were selected based on the S/N (signal-to-noise) ratio. It has been found that cutting speed is the most influential parameter on textured tool performance. It is suggested machining parameters for turning SS 316L with a micro-groove-textured tool at moderate cutting speed, feed, and high depth of cut. The results demonstrate that the micro-groove texture significantly improves tool life and reduces cutting forces compared to non-textured tools, making it a potential solution for sustainable and high-performance machining.

Keywords: Micro-groove texture, high-speed steel, dry turning, SS 316L, tool wear, cutting forces, surface roughness.

1. Introduction

Cutting fluids play a crucial role in machining by reducing friction, tool wear, and cutting temperatures. However, as Graham (2008) reported, using cutting fluids can increase the overall machining cost by up to 15%, not to mention their environmental pollution and health hazards when disposed of improperly. To address these challenges, a sustainable approach is required that eliminates the need for cutting fluids while maintaining effective machining performance [1], [2].

Surface texturing on cutting tools has emerged as a potential solution, offering a way to reduce friction and temperatures by altering the chip-tool interaction. Micro-groove textures, in particular, have shown promising results in minimizing contact areas and entrapping wear debris, ultimately reducing wear and friction. Various studies have demonstrated the improved performance of textured tools in dry machining environments [3], [4].Numerous studies have highlighted the positive impact

of surface texturing on the rake and flank surfaces of cutting tools, demonstrating improvements in cutting performance through reduced cutting pressures and lower temperatures. This texturing not only enhances the tribological properties of tools but also unlocks a range of functional capabilities, making it a promising technique for various machining applications. The adoption of different texture designs and fabrication techniques across tool materials has been a significant focus in recent research, with most studies reporting marked improvements in performance [5], [6].Xie et al. (2013) and Su et al. (2017) conducted studies on the influence of micro-groove textures on cutting tool performance during dry machining of titanium alloys. Their results showed that micro-textures effectively reduced friction and adhesion at the chip-tool interface, leading to a notable reduction in cutting forces and temperatures. This was attributed to the altered chip flow and minimized contact area facilitated by the micro-grooves, which trapped wear debris and improved the cutting process efficiency. In another study by Patel et al. (2019), the influence of micro-groove texture dimensions, including width, spacing, and depth, was analyzed on a tungsten carbide (WC) tool during the orthogonal turning of alloy steel. The findings indicated that groove width and spacing had a significant impact on tool performance, with larger groove dimensions resulting in a decreased chip-tool contact area. This reduction in contact area subsequently lowered the cutting forces, contributing to improved tool life and machining efficiency. [10] The authors observed that micro-groove texture with geometric parameters of width of 75 μm, pitch of 100 μm and distance of 75 μm exhibits better performance. Arulkirubakaran et al. (2018) reduced the cutting forces by up to 30% during the machining of Al-Cu/TiB_2 composite material by using a linearly textured WC tool where textures are oriented perpendicular to chip flow.[11]Rathod et al. (2016) fabricated square and linear textures on WC inserts and observed that the square-textured tool gave better cutting performance than the linear one.[12]Soni&Mashinini (2021) studied the machinability of SS 316 material with a textured WC tool by conducting different turning experiments with different combinations of feed, cutting speed, and depth of cut, respectively.[13] The authors stated that longer tool life is obtained at a higher feed rate, cutting speed, and moderate depth of cut. Prasad & Syed, 2022, reduced the friction coefficient by nearly 14% by using a triangular-shaped spot-textured HSS tool while machining aluminium (6063 T6) alloy.[14]Gajrani et al. (2018) created micro-textures on a plasma nitride HSS tool with a Vickers hardness indentation tester and performed turning experiments on AISI 1040 steel in a solid lubricant environment.[15] Their results revealed that cutting forces and cutting temperature at the chip-tool interface are reduced by the textured tool by up to 41% and 23%, respectively, compared to the conventional cutting tool. Prasad & Syed (2022) improved HSS tool life by nearly 200% by texturing followed by a laser shock peening process while machining SS 316 L materials in a dry environment.[14]Sawant et al. (2018) improved HSS tool performance by fabricating spot and dimple textures on the tool rake face during truing of Ti-6Al-4V material in a dry environment.[16] Roy et al. (2021) examined the influence of machining parameters such as cutting speed and feed on the machinability of aluminium (A1100) alloy during dry turning with a dimple-textured HSS tool. [17] It was revealed that lower values of cutting forces are obtained at high speed and low feed. Similarly, Sasi et al. (2017) and Sugihara et al. (2017) improved HSS tool performance by fabricating dimple textures on its rake face during the orthogonal turning of aluminium alloy.[18] [19]Nagendra Prasad and Ismail (2022) fabricated protruded textures on HSS tool rake faces by reverse EDM and improved tool life up to 110% while dry turning SS 316L material.

2. Materials and Methods

Work piece Material

In this study, austenitic stainless steel (SS) 316L was chosen as the work piece material due to its widespread use in biomedical and food industries, as well as its known machining challenges due to its low thermal conductivity and high toughness. The SS 316L work piece was in the form of a cylindrical round bar with an initial diameter of 38 mm and a length of 350 mm.

Cutting Tool Material

High-speed steel (HSS) of T-42 grade was selected as the cutting tool material for this investigation. The cutting tools were procured from Rohit Tools, Haryana, India. HSS tools are widely known for their ability to withstand high temperatures and wear, making them suitable for machining hard materials such as SS 316L.

Micro-Groove Texturing of Cutting Tools

The micro-groove textures were fabricated on the rake face of the cutting tool using a wire EDM (electro-discharge machining) process. The grooves were oriented perpendicular to the primary cutting edge to minimize friction and enhance cutting performance. The wire EDM process parameters used for fabricating the micro-groove textures are presented in **Table 1**.

Table 1. Process parameters of wire cut EDM to make textures on HSS, Tool geometry and SS 316L composition.

Process parameters of wire cut EDM	**Value**
Peak Current (A)	3
Peak Voltage (V)	150
Spark gap voltage (V)	50
Pulse on-time (µs)	120
Pulse off-time (µs)	60
Wire feed rate (m/min)	4
Wire tension (g)	900
Flushing Pressure (kg/cm^2)	1.5
Tool geometry	**Value**
Back rake angle	8°
Side rake angle	20°
End relief angle	8°
Side relief angle	8°
End cutting edge angle	5°
Side cutting edge angle	10°
SS 316 L Composition (wt.%)	
Cr : 16-18	N : 0.1
Ni : 10-14	Mg : 2
Mo 2-3	Si : 0.75
K : 0.045	C : 0.08
S : 0.03	Fe : Balance

In the current work, cutting speed *(V)*, feed *(f)*, and depth of cut *(Dc)* are considered turning process parameters, and each parameter is varied at three levels. The responses are shear angle, cutting forces, and tool wear as presented in Table 2. A total of nine turning experiments were conducted based on Taguchi's L9 orthogonal array. The cutting forces main cutting force (*Fc*) and thrust force (*Ft*) are measured by 3-axis kistler dynamometer. The 3D optical microscope was used to measure the tool wear and chick thickness. Chip morphology was studied by scanning electron microscope (SEM). Chip thickness ratio (*rc*) and shear angle (ϕ) are calculated by using of *Eq. 1* and *Eq.2*.

$$r_c = \frac{Depth\,of\,cut}{Chip\,Thickness} \tag{1}$$

$$\phi = \tan^{-1}\left(\frac{r_c \cos\alpha}{1 - r_c \sin\alpha}\right) \tag{2}$$

Where $'\alpha'$ is the back rake angle. The experimental set-up and work flow chart is shown in Figure.

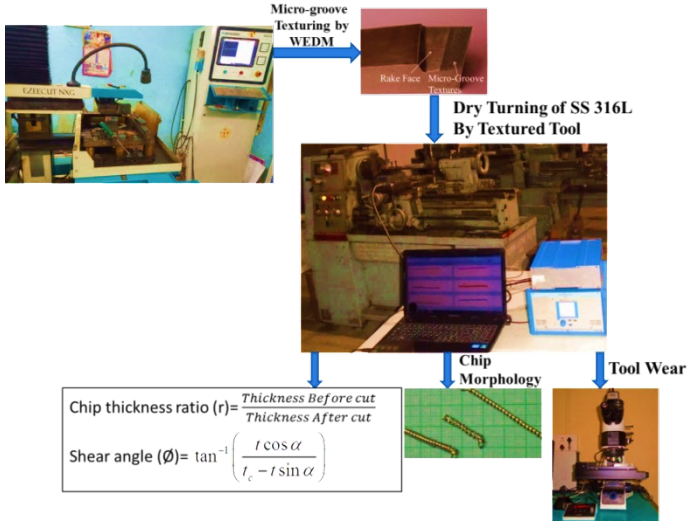

Fig. 1 The work flow chart and experimental set up.

Table 2. Representation of turning experimental conditions and their levels.

Varied parameters and their levels			
Parameter	**Level 1**	**Level 2**	**Level 3**
Cutting Speed, *V* (m/min)	25	32.5	40
Feed, *f* (mm/rev)	0.56	0.103	0.15
Depth of cut, *Dc* (mm)	0.5	0.75	1
Machining Performance output (Response variable)			
Response variable 1	Shear angle, ϕ (°)		
Response variable 2	Cutting force, *Fc* (N)		
Response variable 3	Thrust force, *Ft* (N)		
Response variable 4	Flank wear, *Vb* (μm)		

Table 3 presents Taguchi's L9 orthogonal array experimental design with results. The effect of process parameters and their significance on the responses was studied by Taguchi's *S/N(signal to noise)* ratio. The *S/N* ratio is calculated by *Eq. 3* for *"larger is better,"* and it is considered for shear angle. The *S/N* ratio is calculated by *Eq. 4* for *"smaller is better,"* and it is considered for cutting

forces, tool wear, and surface roughness. The *S/N* ratio values corresponding to each experimental condition is shown in Table 4.

$$\frac{S}{N} = 10 * \log\left(\frac{\sum Y^2}{n}\right) \quad (3)$$

$$\frac{S}{N} = 10 * \log\left(\frac{\sum 1/Y^2}{n}\right) \quad (4)$$

Where *'Y'* is the measured data and *'n'* is the number of experimental data.

Table 3. Taguchi experimental design (L9) conditions and results.

Experiment No.	Cutting Speed, *V* (m/min)	Feed, *f* (mm/rev)	Depth of cut, *Dc* (mm)	Shear angle, ϕ (°)	Cutting force, *Fc* (N)	Thrust force, *Ft* (N)	Flank wear, *Vb* (μm)
1	25	0.056	0.5	23.58	352.65	72.15	313.45
2	25	0.103	0.75	24.35	331.35	62.51	264.34
3	25	0.15	1	22.521	385.65	83.15	323.78
4	32.5	0.056	0.75	29.25	330.35	64.51	195.48
5	32.5	0.103	1	33.42	263.5	49.11	142.25
6	32.5	0.15	0.5	22.82	372.25	76.32	285
7	40	0.056	1	37.52	214.61	32.69	352.25
8	40	0.103	0.5	39.42	185.25	26.87	295.67
9	40	0.15	0.75	36.259	222.15	29.31	465.14

Table 4. Taguchi experimental results and S/N ratio values.

Expt. No.	Shear angle, ϕ (°)		Cutting force, *Fc* (N)		Thrust force, *Ft* (N)		Flank wear, *Vb* (μm)	
	Value	S/N ratio	Value	S/N ratio	Value	S/N ratio	Value	S/N ratio
1	23.58	27.45	352.65	-50.9469	72.15	-37.1647	313.45	-49.9234
2	24.35	27.73	331.35	-50.4057	62.51	-35.9190	264.34	-48.4433
3	22.521	27.05	385.65	-51.7239	83.15	-38.3972	323.78	-50.2050
4	29.25	29.32	330.35	-50.3795	64.51	-36.1925	195.48	-45.8220
5	33.42	30.48	263.5	-48.4156	49.11	-33.8234	142.25	-43.0610
6	22.82	27.16	372.25	-51.4167	76.32	-37.1647	285	-49.0969
7	37.52	31.48	214.61	-46.6330	32.69	-35.9190	352.25	-50.9370
8	39.42	31.91	185.25	-45.3552	26.87	-38.3972	295.67	-49.4161
9	36.259	31.18	222.15	-46.9329	29.31	-36.1925	465.14	-53.3517

3. **Results and Discussion**

3.1 Shear Angle Analysis

The shear angle, a critical factor affecting chip formation and machining efficiency, was calculated for different machining conditions using Eq. 2. The corresponding signal-to-noise (S/N) ratio values are shown in **Table 4**. The shear angle varied significantly across the experiments, ranging from **22° to 39°**, indicating substantial changes in the chip formation process under different machining conditions.

- **Minimum shear angle**: Experiment 3, with a shear angle of 22°, occurred under low cutting speed and moderate feed rates.
- **Maximum shear angle**: Experiment 8, with a shear angle of 39°, was observed at higher cutting speeds and optimized feed and depth of cut parameters.

Effect of Machining Parameters on Shear Angle

Based on the response table for the S/N ratio of shear angle (**Table 5**), it is clear that **cutting speed** is the most influential parameter, with a delta value of **4.12**. This is followed by the **feed rate** and **depth of cut**, which exhibit lower delta values of **1.57** and **0.83**, respectively. These results indicate that increasing cutting speed has a more pronounced effect on the shear angle compared to feed and depth of cut. The optimal levels of machining parameters for achieving the maximum shear angle are as follows:

- **Cutting speed**: 40 m/min (Level 3)
- **Feed rate**: 0.103 mm/rev (Level 2)
- **Depth of cut**: 1 mm (Level 3)

The morphology of chips plays a significant role in understanding the efficiency of the cutting process and is directly related to the shear angle. Figure 3 shows photographic images of the chips produced during the dry turning of SS 316L with textured tools under different machining conditions. **At lower cutting speed (25 m/min), feed (0.15 mm/rev), and depth of cut (0.5 mm),** ribbon-type continuous chips were formed due to the low shear angle. The continuous nature of the chips indicates a less efficient cutting process with more heat generation. **As the depth of cut and feed rate increased,** the chips transitioned into long, continuous shapes. The increased shear angle contributed to better chip evacuation, but the continuous form suggests that the cutting process still retained some inefficiency, such as high tool wear and increased temperatures. **At the highest cutting speed of 40 m/min and feed rate of 0.103 mm/rev**, discontinuous helical chips were observed. This chip morphology is preferred in machining, as it indicates better material removal, less heat generation, and reduced tool wear.

Response Table for S/N Ratio of Shear Angle

Table 5. Response Table for S/N ratio of Shear Angle.

Level	Cutting Speed (m/min)	Feed (mm/rev)	Depth of cut (mm)
01	27.41	29.42	28.84
02	28.99	**30.04**	29.41
03	**31.53**	28.47	**29.67**
Delta	4.12	1.57	0.83

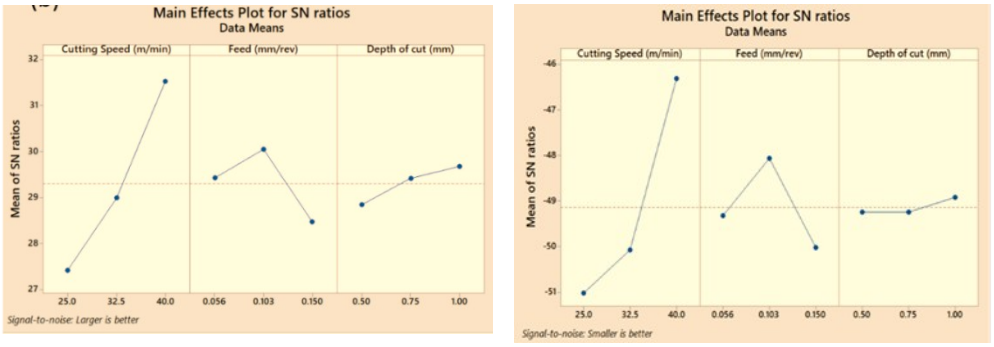

Fig. 2 The main effect plot for S/N ratios of Shear angle.

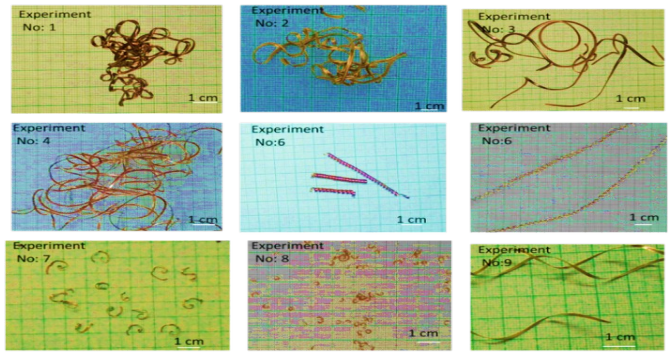

Fig.3 Photographic images of chips while turning of SS 316L with textured tools.

3.2 Cutting force and Thrust force

The cutting and thrust forces at different machining conditions are measured using dynamometer. The values of S/N ratio are show in Table 4. It can be observed that the cutting force is varied from 185-385 based on the experimental conditions. The lower value of cutting force observed during experiment number 8 and maximum for experiment number 3. From the response table (Table 6) it is noticed that the most influential parameter is cutting speed with high *delta* value 4.72 followed by the feed and depth of cut. The optimum parameter levels for lower cutting force are level 1 for cutting speed (25 m/min), level 3 for feed (0.15 mm/rev), and level 1 for depth of cut (0.5 mm) which can be seen from S/N main effect plot. (Figure 4)

Table 6. Response Table for S/N ratio of Cutting and Thrust forces.

	Level	Cutting Speed (m/min)	Feed (mm/rev)	Depth of cut (mm)
Cutting force	01	**-51.03**	-49.32	**-49.24**
	02	-50.07	-48.06	**-49.24**
	03	-46.31	**-50.02**	-48.92
	Delta	4.72	1.97	0.32
	Rank	1	2	3
	Level	**Cutting Speed (m/min)**	**Feed (mm/rev)**	**Depth of cut (mm)**
Thrust force	01	**-37.16**	-36.43	**-37.58**
	02	-35.73	-36.05	-36.10
	03	-36.84	**-37.25**	-36.05
	Delta	1.43	1.20	1.53

Rank	2	3	1

As in the case of cutting force the lower value of thrust force also observed during experiment number 8 and maximum for experiment number 3. From the response table (Table 6) it is noticed that the most influential parameter is depth of cut with high *delta* value 1.53 followed by the cutting speed and feed. The optimum parameter levels for lower thrust force are level 1 for cutting speed (25 m/min), level 3 for feed (0.15 mm/rev), and level 1 for depth of cut (0.5 mm) which can be seen from S/N main effect plot. However, from the results it can be observed that both cutting forces reduce with increase in cutting speed due to thermal softening of the material. Moreover, when feed and depth of cut increases, it causes for increase in material removal this led to increase in energy required for shearing material and results in high cutting forces. As can be observed, the delta of cutting speed is high and ranked as 1 for cutting force and the delta of cutting depth is high and ranked as 1 for thrust force. It suggests that, compared to other machining parameters, cutting speed and depth of cut are the most important parameters to minimize cutting and thrust forces during the turning of 316L SS. As can be seen, experiment number 8 has the lowest S/N ratio, which indicates that the combination of cutting speed of 40 m/min, feed of 0.103 mm/rev, and depth of cut of 1 mm is the most efficient parameter level for reducing cutting forces. Additionally, the S/N ratio main effects plots display a similar pattern of behaviour, as shown in Fig. 4

It can be observed that the flank wear is varied from 142-465µm based on the experimental conditions. The lower value of flank wear was observed during experiment number 5 and maximum for experiment number 9. From the response table (Table 7) it is noticed that the most influential parameter is cutting speed with high *delta* value 5,24 followed by the feed and depth of cut. The optimum parameter levels for minimum flank wear are level 3 for cutting speed (40 m/min), level 3 for feed (0.15 mm/rev), and level 1 for depth of cut (0.5 mm). Which can be seen from S/N main effect plot.

Table 7. Response Table for S/N ratio of Flank Wear.

Level	Cutting Speed (m/min)	Feed (mm/rev)	Depth of cut (mm)
01	-49.52	-48.89	**-49.48**
02	-45.99	-46.97	-49.21
03	**-51.23**	**-50.88**	-48.07
Delta	5.24	3.91	1.41
Rank	1	2	3

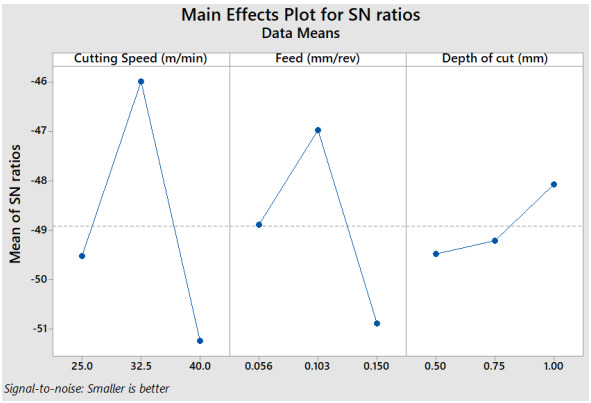

Fig. 5 The main effect plot for S/N ratios of Flank wear.

Generally, the cutting temperature at tool-work interaction is increases with increase in cutting speed this lead to reduce the surface hardness of the material and causes for high flank wear. Therefore, it was observed that maximum flank wear (V_b = 465.14 μm) was occurred with high cutting speed of 40 m/min, feed rate of 0.15 mm/rev and depth of cut of 0.75 mm. Moreover, at low cutting speed of 25 m/min with the different combinations of feed depth of cut also produces more tool wear due to higher machining time which has the high tool and work piece interactions. The minimum flank wear has observed at cutting speed of 32.5 m/min, feed of 0.103 mm/rev and depth of cut of 1 mm.

4. Conclusions

Turning experiments were conducted on SS 316L using micro-groove textured high-speed steel (HSS) tools with different combinations of machining parameters such as cutting speed (V), feed (f), and depth of cut (Dc). The influence of these parameters on the cutting performance was analyzed. The following conclusions can be drawn from the study:

- **Chip Formation**: Increased depth of cut and feed rate results in the formation of long, continuous chips, which can negatively impact machining efficiency.
- **Shear Angle and Chip Shape**: Helical-shaped continuous chips are produced as cutting speed and feed rate increase due to an increase in the shear angle, indicating improved cutting conditions.
- **Discontinuous Chips**: Discontinuous chips, which are preferred in machining due to reduced heat generation and tool wear, were observed at a maximum cutting speed of 40 m/min and a feed rate of 0.103 mm/rev.
- **Optimal Machining Parameters**: The combination of a cutting speed of 40 m/min, feed rate of 0.103 mm/rev, and depth of cut of 1 mm was found to be the most efficient parameter setting for reducing cutting forces and improving tool life.
- **Tool Wear**: Lower cutting speeds, especially 25 m/min, resulted in higher tool wear due to prolonged machining time and increased tool-work piece interaction, highlighting the importance of optimizing cutting speed to minimize wear.
- **Minimum Flank Wear**: The minimum tool wear was observed at a cutting speed of 32.5 m/min, feed rate of 0.103 mm/rev, and depth of cut of 1 mm, indicating that these parameters are optimal for tool longevity.

These findings provide valuable insights into the effects of micro-groove textured tools and machining parameters on the performance during dry turning of SS 316L. The results support the use of higher cutting speeds and moderate feed rates to enhance machining efficiency while reducing tool wear.

References

[1] Graham T. Smith, “Cutting fluids,” in *Cutting Tool Technology*, Graham T. Smith, Ed., Southampton, UK: Springer, London, (2008), pp. 38–430. doi: 10.1007/978-3-662-53120-4_6397.

[2] S. Debnath, M. M. Reddy, and Q. S. Yi, “Environmental friendly cutting fluids and cooling techniques in machining: A review,” *J. Clean. Prod.*, vol. 83, pp. 33–47, (2014), doi: 10.1016/j.jclepro.2014.07.071.

[3] A. R. Machado *et al.*, “State of the art of tool texturing in machining,” *J. Mater. Process. Technol.*, vol. 293, no. June 2020, p. 117096, (2021), doi: 10.1016/j.jmatprotec.2021.117096.

[4] T. Sugihara and T. Enomoto, “Performance of cutting tools with dimple textured surfaces: A comparative study of different texture patterns,” *Precis. Eng.*, vol. 49, pp. 52–60, (Jul. 2017), doi: 10.1016/j.precisioneng.2017.01.009.

[5] P. Ranjan and S. S. Hiremath, “Role of textured tool in improving machining performance: A review,” *Journal of Manufacturing Processes*, vol. 43. Elsevier Ltd, pp. 47–73, Jul. 01, (2019). doi: 10.1016/j.jmapro.2019.04.011.

[6] K. N. Prasad, I. Syed, and S. K. Subbu, “Laser dimple texturing–applications, process, challenges, and recent developments: a review,” *Australian Journal of Mechanical Engineering*, vol. 20, no. 2. Taylor and Francis Ltd., pp. 316–331, (2022). doi: 10.1080/14484846.2019.1705533.

[7] J. Xie, M. J. Luo, K. K. Wu, L. F. Yang, and D. H. Li, “Experimental study on cutting temperature and cutting force in dry turning of titanium alloy using a non-coated micro-grooved tool,” *Int. J. Mach. Tools Manuf.*, vol. 73, pp. 25–36, (2013), doi: 10.1016/j.ijmachtools.2013.05.006.

[8] Y. Su, Z. Li, L. Li, J. Wang, H. Gao, and G. Wang, “Cutting performance of micro-textured polycrystalline diamond tool in dry cutting,” *J. Manuf. Process.*, vol. 27, pp. 1–7, (2017), doi: 10.1016/j.jmapro.2017.03.013.

[9] K. V. Patel, S. R. Shah, and T. Özel, “Orthogonal cutting of alloy steel 4340 with micro-grooved cutting tools,” *Procedia CIRP*, vol. 82, no. March, pp. 178–183, (2019), doi: 10.1016/j.procir.2019.03.276.

[10] Y. Liu *et al.*, “Effect of texture parameters on cutting performance of flank-faced textured carbide tools in dry cutting of green Al2O3 ceramics,” *Ceram. Int.*, vol. 44, no. 11, pp. 13205–13217, (2018), doi: 10.1016/j.ceramint.2018.04.146.

[11] D. Arulkirubakaran, V. Senthilkumar, S. Dinesh, C. Velmurugan, N. Manikandan, and R. Raju, “Effect of Textured Tools on Machining of Ti-6Al-4V Alloy under Lubricant Condition,” *Mater. Today Proc.*, vol. 5, pp. 14230–14236, (2018). Available: www.sciencedirect.comwww.materialstoday.com/proceedings

[12] P. Rathod, S. Aravindan, and Venkateswara Rao P., “Performance Evaluation of Novel Micro-textured Tools in Improving the Machinability of Aluminum Alloy (Al 6063),” *Procedia Technol.*, vol. 23, pp. 296–303, (2016), doi: 10.1016/j.protcy.2016.03.030.

[13] H. Soni and P. M. Mashinini, “An Analysis on Tool-Chip Interaction During Dry Machining of SS316 Using Textured Carbide Tools,” *Arab. J. Sci. Eng.*, vol. 46, no. 8, pp. 7611–7621, (2021), doi: 10.1007/s13369-021-05499-6.

[14] K. N. Prasad and I. Syed, “Surface Texturing and Laser Shock Peening Processes on High-Speed Steel Tool for Sustainable Machining,” *Arab. J. Sci. Eng.*, vol. 47, no. 7, pp. 8589–8600, (2022), doi: 10.1007/s13369-021-06367-z.

[15] K. K. Gajrani, S. Suresh, and M. R. Sankar, “Environmental friendly hard machining performance of uncoated and MoS2 coated mechanical micro-textured tungsten carbide cutting tools,” *Tribol. Int.*, vol. 125, no. April, pp. 141–155, (2018), doi: 10.1016/j.triboint.2018.04.031.

[16] M. S. Sawant, N. K. Jain, and I. A. Palani, “Influence of dimple and spot-texturing of HSS cutting tool on machining of Ti-6Al-4V,” *J. Mater. Process. Technol.*, vol. 261, no. February, pp. 1–11, (2018), doi: 10.1016/j.jmatprotec.2018.05.032.

[17] R. S. Roy, S. Dash, T. R. Mahapatra, D. Mishra, and S. Jaypuria, “Cutting Performance Analysis of Surface Textured Tools in Dry Turning: Optimisation of process parameters,” *E3S Web Conf.*, vol. 309, (2021), doi: 10.1051/e3sconf/202130901164.

[18] R. Sasi, S. Kanmani Subbu, and I. A. Palani, “Performance of laser surface textured high speed steel cutting tool in machining of Al7075-T6 aerospace alloy,” *Surf. Coatings Technol.*, vol. 313, pp. 337–346, (2017), doi: 10.1016/j.surfcoat.2017.01.118.

[19] T. Sugihara, P. Singh, and T. Enomoto, “Development of novel cutting tools with dimple textured surfaces for dry machining of aluminum alloys,” in *Procedia Manufacturing*, Elsevier B.V(2017), pp. 111–117. doi: 10.1016/j.promfg.2017.11.013.

[20] K. Nagendra Prasad and S. Ismail, “Machining performance of protruded textured high-speed steel cutting tool under dry turning operation,” *Mater. Today Proc.*, vol. 66, pp. 2115–2123, Jan. (2022), doi: 10.1016/j.matpr.2022.05.559.

[21] D. Vasumathy and A. Meena, “Influence of micro scale textured tools on tribological

properties at tool-chip interface in turning AISI 316 austenitic stainless steel," *Wear*, vol. 376–377, pp. 1747–1758, (2017), doi: 10.1016/j.wear.2017.01.024.

[22] P. M. Mashinini, H. Soni, and K. Gupta, "Investigation on dry machining of stainless steel 316 using textured tungsten carbide tools," *Mater. Res. Express*, vol. 7, no. 1, (2020), doi: 10.1088/2053-1591/ab5630.

[23] A. I. Fernández-Abia, J. Barreiro, L. N. L. De Lacalle, and S. Martínez, "Effect of very high cutting speeds on shearing, cutting forces and roughness in dry turning of austenitic stainless steels," *Int. J. Adv. Manuf. Technol.*, vol. 57, no. 1–4, pp. 61–71, (2011), doi: 10.1007/s00170-011-3267-9.

[24] H.-B. He et al., (2017)"A study on major factors influencing dry cutting temperature of AISI 304 stainless steel," International Journal of Precision Engineering and Manufacturing, vol. 18, no. 10, pp. 1387–1392.